


# Engineered Stem Cells Improve Neurogenic Bladder by Overexpressing SDF-1 in a Pelvic Nerve Injury Rat Model

Cell Transplantation  
Volume 29: 1–12  
© The Author(s) 2020  
Article reuse guidelines:  
sagepub.com/journals-permissions  
DOI: 10.1177/0963689720902466  
journals.sagepub.com/home/ctj  


Guan Qun Zhu<sup>1,2</sup> , Seung Hwan Jeon<sup>1,2</sup>, Kyu Won Lee<sup>1</sup>, Hyuk Jin Cho<sup>1</sup>, U-Syn Ha<sup>1</sup>, Sung-Hoo Hong<sup>1</sup>, Ji Youl Lee<sup>1</sup>, Eun Bi Kwon<sup>1,2</sup>, Hyo-Jin Kim<sup>3</sup>, Soon Min Lee<sup>3</sup>, Hey-Yon Kim<sup>3</sup>, Sae Woong Kim<sup>1,2</sup>, and Woong Jin Bae<sup>1,2</sup>

## Abstract

There is still a lack of sufficient research on the mechanism behind neurogenic bladder (NB) treatment. The aim of this study was to explore the effect of overexpressed stromal cell-derived factor-1 (SDF-1) secreted by engineered immortalized mesenchymal stem cells (imMSCs) on the NB. In this study, primary bone marrow mesenchymal stem cells (BM-MSCs) were transfected into immortalized upregulated SDF-1-engineered BM-MSCs (imMSCs/eSDF-1<sup>+</sup>) or immortalized normal SDF-1-engineered BM-MSCs (imMSCs/eSDF-1<sup>-</sup>). NB rats induced by bilateral pelvic nerve (PN) transection were treated with imMSCs/eSDF-1<sup>+</sup>, imMSCs/eSDF-1<sup>-</sup>, or sham. After a 4-week treatment, the bladder function was assessed by cystometry and voiding pattern analysis. The PN and bladder tissues were evaluated via immunostaining and western blotting analysis. We found that imMSCs/eSDF-1<sup>+</sup> expressed higher levels of SDF-1 in vitro and in vivo. The treatment of imMSCs/eSDF-1<sup>+</sup> improved NB and evidently stimulated the recovery of bladder wall in NB rats. The recovery of injured nerve was more effective in the NB+imMSCs/eSDF-1<sup>+</sup> group than in other groups. High SDF-1 expression improved the levels of vascular endothelial growth factor and basic fibroblast growth factor. Apoptosis was decreased after imMSCs injection, and was detected rarely in the NB+imMSCs/eSDF-1<sup>+</sup> group. Injection of imMSCs boosted the expression of neuronal nitric oxide synthase, p-AKT, and p-ERK in the NB+imMSCs/eSDF-1<sup>+</sup> group than in other groups. Our findings demonstrated that overexpression of SDF-1 induced additional MSC homing to the injured tissue, which improved the NB by accelerating the restoration of injured nerve in a rat model.

## Keywords

neurogenic bladder, mesenchymal stem cells, gene regulation, SDF-1 overexpression, homing

## Introduction

Neurogenic bladder (NB) is a vexing problem for both the patients and the urologists<sup>1</sup>. As is well known, NB is not a homogeneous entity, but a widely used term to denote lower urinary tract dysfunction, which is a common complication of neurological disease following surgical treatment of pelvic neoplasms<sup>2</sup>. The symptoms involve frequent urination, urinary incontinence, voiding by abdominal straining, and urinary retention<sup>3</sup>. Currently, the primary goals of NB management include protection of the upper urinary tract function and restoration of bladder dysfunction<sup>4</sup>. However, the mechanism underlying NB treatment is still not fully understood.

Mesenchymal stem cells (MSCs) represent a novel and potential therapeutic strategy with convincing and promising

<sup>1</sup> Department of Urology, College of Medicine, The Catholic University of Korea, Seoul, Republic of Korea

<sup>2</sup> Catholic Integrative Medicine Research Institute, The Catholic University of Korea, Seoul, Republic of Korea

<sup>3</sup> Department of Stem Cell Therapy, SL BIGEN, Seongnam, Republic of Korea

Submitted: August 8, 2019. Revised: November 6, 2019. Accepted: December 10, 2019.

### Corresponding Authors:

Woong Jin Bae and Sae Woong Kim, Department of Urology, College of Medicine, The Catholic University of Korea, 222, Banpo-daero, Seocho-gu, Seoul 06591, Republic of Korea.

Emails: bwoong@catholic.ac.kr; ksw1227@catholic.ac.kr



evidence in many medical fields<sup>5-7</sup>. Currently, stem cell therapy has evolved from animal experiments to clinical settings<sup>8</sup>, which indicates their safety and effectiveness. In our previous study<sup>9</sup>, we found that MSC therapy accelerated the recovery of injured nerve and tissue. Therefore, we believe that MSC therapy is effective in NB treatment. Immortalized stem cells were selected for experimental use for increased accuracy<sup>10,11</sup>, because immortalized mesenchymal stem cells (imMSCs) exhibit higher proliferation and anti-senescence ability, compared with general MSCs.

In a recent study, researchers found that stromal cell-derived factor-1 (SDF-1) induced stem cells to recruit endothelial cells, which contributed to vascular pericytes<sup>12</sup>. In our previous experiment, we found that SDF-1 was active during the whole period of tissue recovery and angiogenesis<sup>9</sup>. Therefore, we wondered whether NB can be ameliorated effectively under a high SDF-1 microenvironment. We utilized genetic engineering technology to overexpress SDF-1 to treat the NB in a rat model.

In this study, we developed a rat model of NB via bilateral pelvic nerve (PN) transection, and analyzed the effect of high SDF-1 on NB via upregulation of SDF-1-engineered imMSCs. We hypothesized that upregulated SDF-1 in imMSCs might improve NB function and restore bladder wall efficiently by promoting angiogenesis, tissue regeneration, and nerve recovery.

## Materials and Methods

### Cell Culture and Preparation

Primary bone marrow mesenchymal stem cells (BM-MSCs) were obtained from Catholic Institute of Cell Therapy (CIC, Seoul, Korea), were cultured in low glucose-containing Dulbecco's modified Eagle's medium (Gibco, Waltham, MA, USA) supplemented with 20% fetal bovine serum (Gibco, Waltham, MA, Gibco) and 5 ng/ml basic fibroblast growth factor (bFGF, Cell Signaling Technology, Danvers, MA, USA) at 37°C and 5% CO<sub>2</sub>. To generate upregulated SDF-1-engineered imMSCs, c-myc, hTERT, tetracycline transactivator, and SDF-1 genes were synthesized and transfected with pBD lentiviral vector (SL-BIGEN, Seongnam, Korea). In brief, the reference sequence of SDF-1 was NM\_000609<sup>6</sup>. We designed an optimized DNA sequence to introduce into a vector (Genscript, Nanjing, China). DNA sequencing was performed to confirm the accuracy of the right reading frame of the introduced sequence (Cosmo Genetech, Seoul, Korea). After transfection, cells were seeded on 12-well plates, at a density of  $5 \times 10^5$  cells per well. After 48 h, the supernatant was harvested. The SDF-1 protein level was measured. The SDF-1 expression level was about 10 ng/ml. Immortalized, upregulated SDF-1-engineered BM-MSCs (imMSCs/eSDF-1<sup>+</sup>) were selected monoclonally using antibiotics. Selected imMSCs/eSDF-1<sup>+</sup> were isolated from the cell population using the limiting dilution method.

Meanwhile, vectors without SDF-1 gene were administered into BM-MSCs (imMSCs/eSDF-1<sup>-</sup>) as a control.

### ELISA

BM-MSCs, imMSCs/eSDF-1<sup>-</sup>, and imMSCs/eSDF-1<sup>+</sup> were seeded in 100 mm culture dishes. After full attachment, the completed growth media were removed and cells were washed with phosphate-buffered saline (PBS) three times. Subsequently, 10 ml of fresh serum-free basal media was refilled, and incubated at 37°C in 5% CO<sub>2</sub> for 3 days. The collected media were centrifuged at 3,000 rpm and 4°C for 15 min. The supernatant collected from BM-MSCs, imMSCs/eSDF-1<sup>-</sup>, and imMSCs/eSDF-1<sup>+</sup> conditioned media (CM) was used to examine the SDF-1 in each group by ELISA (R&D Systems Europe, Abingdon, UK) according to the manufacturer's protocol. Meanwhile for comparison, we stained BM-MSCs, imMSCs/eSDF-1<sup>-</sup>, and imMSCs/eSDF-1<sup>+</sup> by Cell Tracker™ CM-DiI (Molecular Probes, Eugene, OR, USA). Then the same ELISA process proceeded in staining group. Absorbance was read at a wavelength of 450 nm in a microplate reader (Synergy H1 M; Biotek, Winooski, VT, USA). At least three separate dishes of cells were assayed for each clone.

### Experimental Animal and Study Design

All animal experiments in this study were approved by the Institutional Animal Care and Use Committee of the Catholic University of Korea (CUMC-2016-0218-01). The 12-week-old male Sprague-Dawley rats, each weighing about 370 to 400 g, were purchased from Orient Bio Co (Orient Bio Co., Seongnam, Korea), and separated into three experimental groups (NB, NB+imMSCs/eSDF-1<sup>-</sup>, and NB+imMSCs/eSDF-1<sup>+</sup>) and 1 sham control group with 12 rats each. The major pelvic ganglion and PN of rats were identified under anesthesia. Rats in the three experimental groups were subjected to PN transection as described previously<sup>13</sup>. The sham control group received sham surgery. After surgery, the rats were housed individually and supplied with freely available food and water.

### MSC Treatment

One week after the NB model was established, rats in the NB+imMSCs/eSDF-1<sup>-</sup> and NB+imMSCs/eSDF-1<sup>+</sup> groups were treated with imMSCs/eSDF-1<sup>-</sup> and imMSCs/eSDF-1<sup>+</sup>, via bilateral PN perineural injection under anesthesia ( $1 \times 10^6$  MSCs diluted in PBS) as described previously<sup>14</sup>. Rats in NB and sham control group were injected with equal volumes of saline. To track the location, of administered imMSCs, they were labeled with Cell Tracker™ CM-DiI before injection according to the manufacturer's protocol.

### Voiding Pattern Analysis

For voiding pattern analysis, rats were individually housed in metabolic cages with a grid at the bottom, and a filter paper below the grid to collect the urine for 3 h. Filter papers were photographed under ultraviolet light and analyzed using the Image J software (NIH, Bethesda, MD, USA) to identify the surface area of the individual voiding spots. The number of spots was defined as the voiding frequency, and 50  $\mu$ l urine was considered equal to 2.8 cm<sup>2</sup> on the filter paper. Voiding pattern analysis was conducted before and after treatment.

### Cystometry

Cystometry experiments were performed in all rats at week 4 after the treatment. In brief, rats were anesthetized using a subcutaneous injection of 1.2 mg/kg of urethane. A suprapubic midline laparotomy was performed to expose the bladder, and a 25-gauge needle connected to a polyethylene tubing was inserted into the bladder through the bladder dome. The tubing was connected to a pressure transducer and a Harvard syringe pump via a three-way stopcock to record intravesical pressure and to infuse saline into the bladder. After emptying the bladder, cystometry was performed using a saline infusion at a rate of 0.04 ml/min. The contraction interval and the contraction pressure (maximum bladder pressure during voiding) were recorded using a polygraph (Grass 7D; Grass Institute Co., Quincy, MA, USA). Nonvoiding contractions (NVCs) were determined during the 2 to 4 min before each voiding contraction. NVCs were defined as contractions >4 cm H<sub>2</sub>O from the baseline pressure during bladder filling. After cystometry, PN and bladder were collected for immunofluorescence staining and western blot analysis.

### Histology and Immunofluorescence Staining

The collected PN and bladder were fixed in 4% paraformaldehyde for 24 h at 4°C before creating a paraffin block, as described previously<sup>9</sup>. The primary antibodies were used as follows: vascular endothelial growth factor (VEGF; diluted 1:200; Santa Cruz Biotechnologies, Santa Cruz, CA, USA),  $\beta$ III-tubulin (diluted 1:200; Abcam, Cambridge, UK), bFGF (diluted 1:500; Cell Signaling Technology, Danvers, MA, USA), SDF-1 (diluted 1:200; Abcam, Cambridge, UK), poly-ADP-ribose polymerase (PARP, diluted 1:500; Abcam, Cambridge, UK), and 6-diamidino-2-phenylindole (DAPI; Vector Laboratories, Inc., Burlingame, CA, USA) were used to stain the nuclei. Digital images were obtained using a Zeiss LSM 510 Meta confocal microscope (Zeiss, Oberkochen, Germany), and bladder images were analyzed using ZEN 2012 (Zeiss, Oberkochen, Germany). The other resulting images were analyzed using Image J to determine the positive rate for each figure. In brief, we used Image J to split each color from merged figure, calculate the intensity of each color,

and then added them. The positive was the ratio of a special color fluorescence intensity to all colors intensity.

### Masson Staining

To evaluate the proportion of collagen and smooth muscle, the bladder walls of rats in each group were stained with Masson trichrome. Bladder wall sections were deparaffinized, rehydrated with graded alcohols, immersed in warm Bouin's solution (Sigma, St. Louis, MO, USA) (55 to 60°C) for 2 h and washed under running tap water for 2 min followed by distilled water for 30 to 60 s. They were stained with Weigert Hematoxylin (Merck, Darmstadt, Germany) for 10 min and washed out. Subsequently, the smooth muscle was stained red with Biebrich Scarlet-Acid-Fuchsin (Sigma, St. Louis, MO, USA) for 10 min, rinsed and immersed in phosphomolybdic phosphotungstic acid (Sigma, St. Louis, MO, USA) for 15 min. The collagen was stained blue with Aniline Blue (Sigma, St. Louis, MO, USA) for 10 min and rinsed in distilled water followed by immersion in 1% acetic acid for 5 min. Finally, the tissues were rehydrated with 100% ethanol, left to air dry and mounted. All sections of bladder tissue were stained at the same time.

### Analysis of Apoptosis In Vivo

We assessed the apoptosis in PN using an immunostaining kit to determine the PARP levels as described previously<sup>9</sup>. The antibodies to PARP along with other primary antibodies are listed in the Histology and Immunofluorescence Staining section.

### Western Blot

Western blot was performed as previously described<sup>9</sup>. In brief, the collected tissue was homogenized using ice-cold RIPA buffer (Cell Signaling Technology, Danvers, MA, USA) containing EDTA-free protease inhibitor cocktail. The phosphatase inhibitor cocktail (Roche Diagnostics GmbH, Basel, Switzerland) and particulate mass were removed by centrifugation (15,000g) for 15 min at 4°C. The supernatants were analyzed by sodium dodecyl sulfate-polyacrylamide gel electrophoresis. The primary antibodies included neuronal nitric oxide synthase (nNOS, diluted 1:200; Santa Cruz Biotechnologies), AKT (diluted 1:200; Cell Signaling Technology, Danvers, MA, USA), p-AKT (diluted 1:200; Cell Signaling Technology, Danvers, MA, USA), p-ERK (diluted 1:200; Cell Signaling Technology, Danvers, MA, USA), SDF-1 (diluted 1:500; Cell Signaling Technology, Danvers, MA, USA), and  $\beta$ -actin (diluted 1:1,000; Abcam, Cambridge, UK).

### Statistical Analysis

All data are presented as mean  $\pm$  standard error and analyzed using SPSS version 22.0 software (SPSS Inc., Chicago, IL, USA). Student's *t*-test and one-way analysis of variance (ANOVA) or two-way ANOVA (followed by Bonferroni post hoc tests) as appropriate were used to evaluate

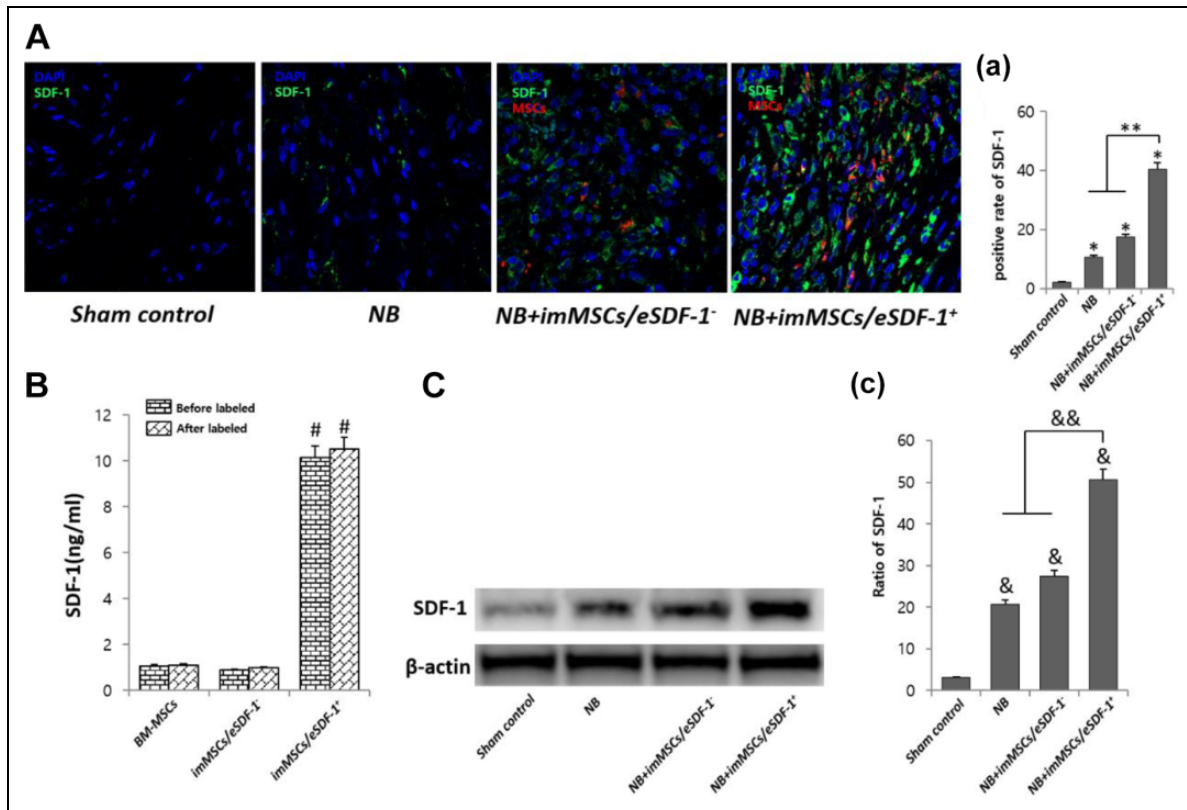


**Fig. 1.** ImMSCs/eSDF-1<sup>+</sup> make a higher SDF-1 microenvironment in vitro and in vivo. (A) Representative images of SDF-1 stain in PN for each group. Original magnification:  $\times 200$ . (a) Positive rate of SDF-1 for each group. Each bar shows the mean values (standard deviation). \* $P < 0.01$ , compared with sham control group. \*\* $P < 0.01$  compared with NB and NB+imMSCs/eSDF-1<sup>-</sup> group. (B) SDF-1 concentration of each group in vitro by ELISA before and after labeled by Cell, Tracker CM-Dil. # $P < 0.01$  compared with other groups. (C) SDF-1 expression of each group in PN using western blot. (c) Quantity analysis of western blot. & $P < 0.01$  compared with sham control group. && $P < 0.01$  compared with NB and NB+imMSCs/eSDF-1<sup>-</sup> groups. imMSC: immortalized mesenchymal stem cell; NB: neurogenic bladder; PN: pelvic nerve; SDF-1: stromal cell-derived factor-1.

the significant differences among groups.  $P < 0.05$  was considered statistically significant.

## Results

### imMSCs/eSDF-1<sup>+</sup> Express Higher SDF-1 In Vitro and Vivo

As shown in Figure 1(A, a) imMSCs/eSDF-1<sup>+</sup> expressed higher levels of SDF-1 in an NB rat model ( $P < 0.01$ ). However, in the control group, reduced levels of SDF-1 were expressed in the PN ( $P < 0.01$ ), suggesting that injury induced SDF-1 expression in vivo. As shown in Figure 1(B), ELISA results indicate that imMSCs/eSDF-1<sup>+</sup> expressed higher levels of SDF-1 in vitro ( $P < 0.01$ ). However, there was no statistically significant difference in the SDF-1 expression of BM-MSCs and imMSCs/eSDF-1<sup>-</sup> groups, which demonstrates that vectors used in transfection have no influence on the SDF-1 expression. As shown in Figure 1(C), in the sham control group, less SDF-1 was expressed in the PN ( $P < 0.01$ ) and the imMSCs/eSDF-1<sup>+</sup> overexpressed SDF-1 in PN ( $P < 0.01$ ).

### imMSCs/eSDF-1<sup>+</sup> Improves NB Significantly

The result of cystometry (Figure 2A) in NB group was apparently better than other groups. As shown in Figure 2(B and C), the mean pressure of the voiding contractions and intermicturition interval in each group varied. The bladders of NB+imMSCs/eSDF-1<sup>-</sup> group and NB+imMSCs/eSDF-1<sup>+</sup> group showed better results ( $P < 0.01$ ), whereas NB+imMSCs/eSDF-1<sup>+</sup> group was better than NB+imMSCs/eSDF-1<sup>-</sup> group ( $P < 0.05$ ). The results of voided volume and voiding frequency before and after treatment are presented in Figure 2(D and E). As shown in Figure 2, imMSC treatment efficiently improved NB, especially in a high SDF-1 environment.

### MSCs Treatment Stimulates the Bladder Recovery Especially in a High SDF-1 Microenvironment

During the 4-week treatment, the bladder wall was assessed by Masson staining. As shown in Figure 3(A and B), the smooth muscle of bladder wall was thicker after MSC treatment ( $P < 0.01$ ). The smooth muscle in the

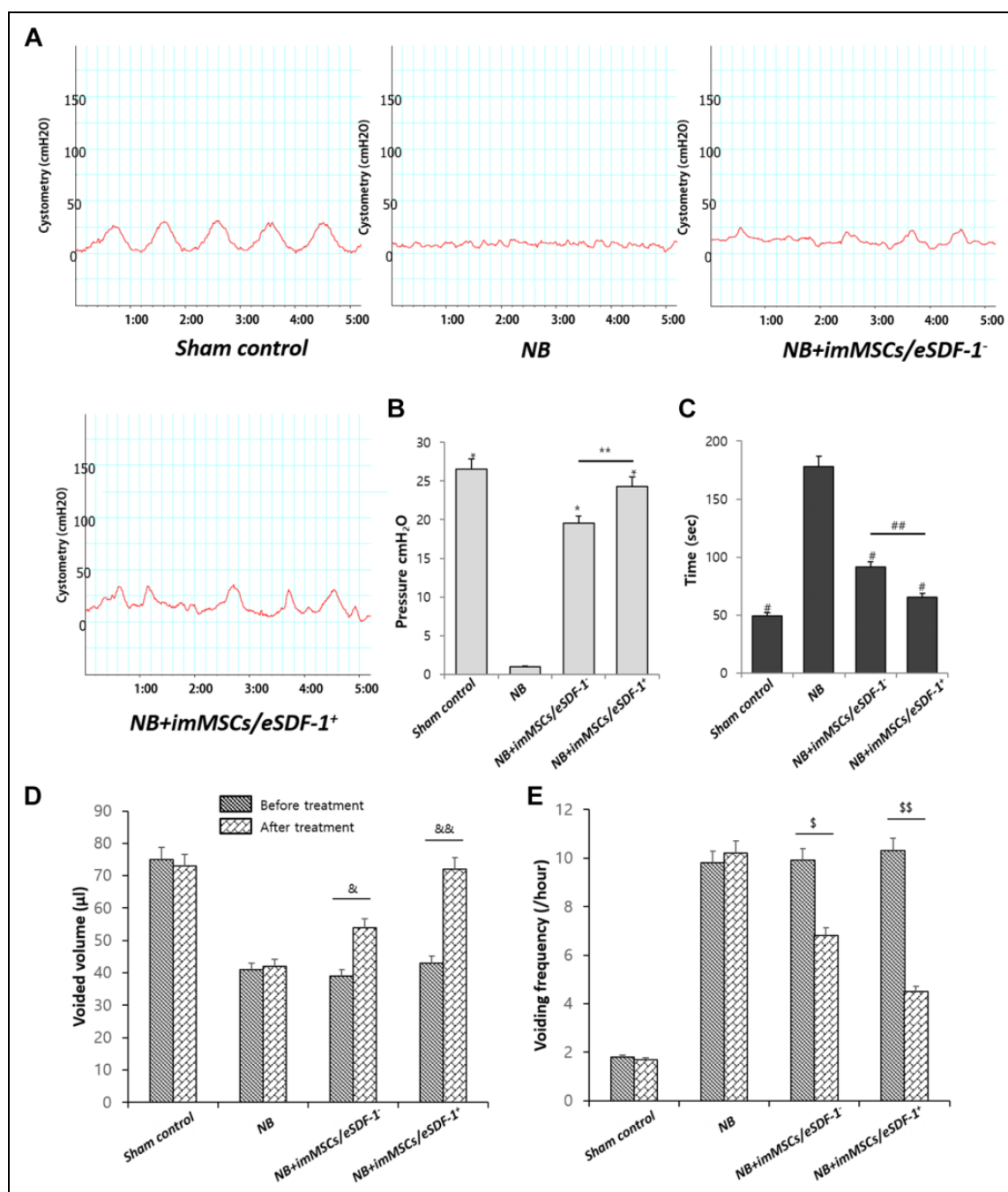


**Fig. 2.** (A) Representative images of cystometry in each group. Sham control is the normal control group. NB means neurogenic bladder. ImMSCs/eSDF-1<sup>+</sup> are high SDF-1-expressing engineered MSCs, and NB+imMSCs/eSDF-1<sup>-</sup> are engineered MSCs transfected by empty vectors. (B) Mean pressure of the voiding contractions compared in each group. \* $P < 0.01$  compared with NB control group. \*\* $P < 0.05$  compared with NB+imMSCs/eSDF-1<sup>-</sup> group. (C) Mean intermicturition interval in each group. # $P < 0.01$  compared with NB control group. ## $P < 0.05$  compared with NB+imMSCs/eSDF-1<sup>-</sup> group. (D) Voided volume and (E) voiding frequency results before and after treatment in each group. &  $P < 0.05$  in the pre- and post-treatment comparison. &&  $P < 0.01$  in the pre- and post-treatment comparison. imMSC: immortalized mesenchymal stem cell; NB: neurogenic bladder; SDF-1: stromal cell-derived factor-1.

NB+imMSCs/eSDF-1<sup>+</sup> group was more than in NB+imMSCs/eSDF-1<sup>-</sup> group ( $P < 0.05$ ), which suggests a more efficient recovery of NB in a high SDF-1 micro-environment (Figure 3B). Figure 3(C) displays the whole profiles of bladders after 2 h of water fasting. The bladder

weight/body weight ratio was maintained for accurate assessment in Figure 3(D). Bladder with imMSCs/eSDF-1<sup>+</sup> treatment showed satisfactory regeneration compared with imMSCs/eSDF-1<sup>-</sup> treatment ( $P < 0.05$ ) and non-treatment ( $P < 0.01$ ).



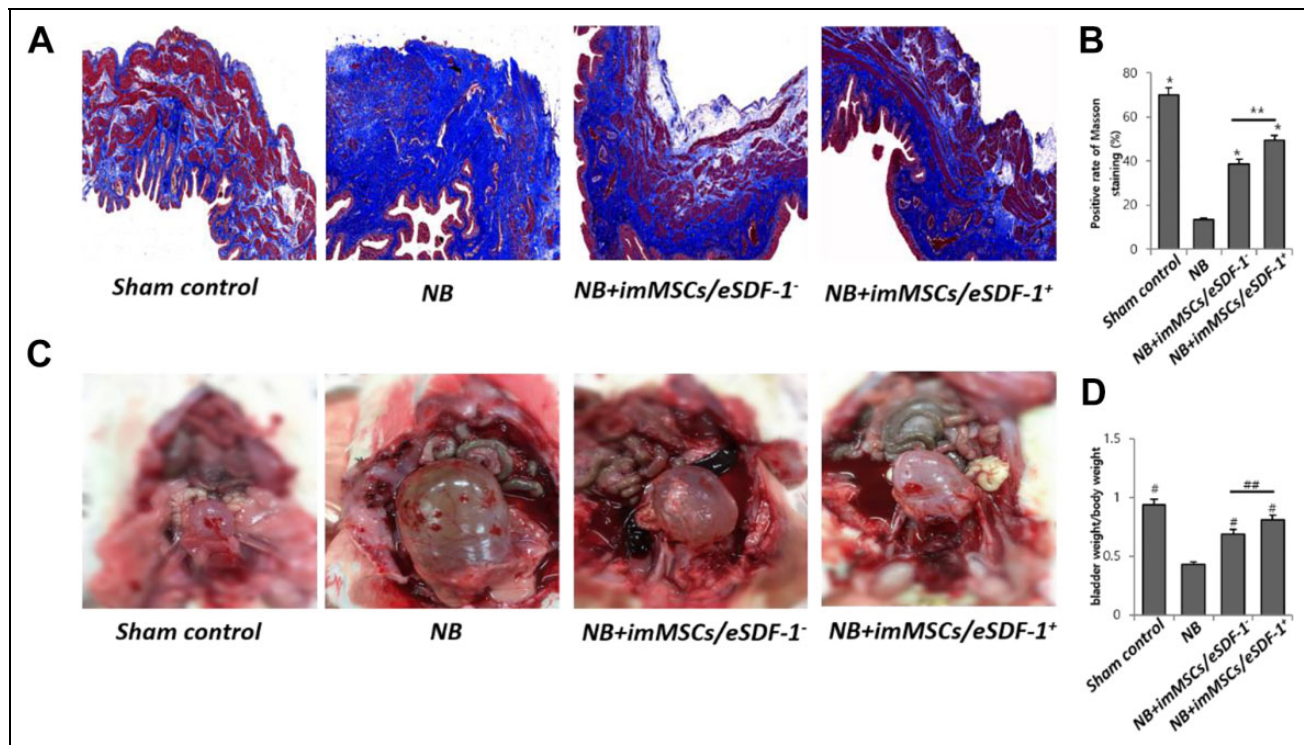


**Fig. 3.** (A) Representative images of Masson Trichrome stain for each group. Red is smooth muscle, and blue is collagen. Original magnification:  $\times 200$ . (B) Percentage area of smooth muscle for each group. Each bar shows the mean values (standard deviation).  $*P < 0.01$  compared with NB group.  $**P < 0.05$  compared with NB+imMSCs/eSDF-1<sup>-</sup> group. (C) Image of rat's bladder in each group after fasting water for 2 h. (D) Bladder, weight/body weight ratio of each group in mg/g.  $^{\#}P < 0.01$  compared with NB group.  $^{\#\#}P < 0.05$  compared with NB+imMSCs/eSDF-1<sup>-</sup> group. imMSC: immortalized mesenchymal stem cell; NB: neurogenic bladder; SDF-1: stromal cell-derived factor-1.

### SDF-1 Induces MSC Homing and Subsequently Improves the Regeneration of Injured PN

As shown in Figure 4(A), nerve recovery was accelerated by imMSC injection. As suggested in Figure 4(B), the nerve volume in NB group was less than in others ( $P < 0.01$ ). The results showed that the nerve in NB+imMSCs/eSDF-1<sup>+</sup> group was higher than in NB+imMSCs/eSDF-1<sup>-</sup> group ( $P < 0.05$ ). Combined with Figure 1(a), we concluded that NB+imMSCs/eSDF-1<sup>+</sup> induced a higher SDF-1 microenvironment around the injured nerve, and accelerated the nerve recovery. Figure 4(C) suggests that the number of imMSCs in NB+imMSCs/eSDF-1<sup>+</sup> group was higher than in NB+imMSCs/eSDF-1<sup>-</sup> group ( $P < 0.05$ ). Meanwhile, 7A and 7B showed a higher nNOS expression in NB+imMSCs/eSDF-1<sup>+</sup> group compared to other groups ( $P < 0.05$ ), which also proved there were more regenerated nerve after imMSCs/eSDF-1<sup>+</sup> injection.

### High SDF-1 Expression Improves the Quantity of VEGF and bFGF

Figure 5(A) shows that imMSCs increase VEGF expression. As depicted in Figure 5(B), imMSCs improve bFGF expression. Figure 5(a and b) shows that the levels of VEGF and bFGF in the NB+imMSCs/eSDF-1<sup>-</sup> and NB+imMSCs/eSDF-1<sup>+</sup> group

were higher than in the NB group ( $P < 0.01$ ). The VEGF and bFGF levels in the NB+imMSCs/eSDF-1<sup>+</sup> group were higher than in the NB+imMSCs/eSDF-1<sup>-</sup> group. In conjunction with Figure 1(a), we conclude that in a higher SDF-1 microenvironment, the expression of VEGF and bFGF was increased. The stimulation of SDF-1, cell viability, and movement require additional growth factors such as VEGF and bFGF.

### Apoptosis Decreases with MSC Injection Especially in a High SDF-1 Microenvironment

As shown in Figure 6(A), without MSCs the apoptosis in the damaged PN was high. However, after imMSC injection the apoptosis was improved. Figure 6(B) displays a positive rate of PARP in each group. We found a higher degree of apoptosis in the NB group ( $P < 0.01$ ). Furthermore, the apoptosis in the NB+imMSCs/eSDF-1<sup>+</sup> group was higher than in the NB+imMSCs/eSDF-1<sup>-</sup> group, which suggested that apoptosis was reduced in a high SDF-1 microenvironment.

### MSCs activate PI3K/AKT/mTOR and MAPK Signaling Pathway via enhanced SDF-1 Expression

In the first study investigating nerve recovery in a high SDF-1 microenvironment, we identified the underlying

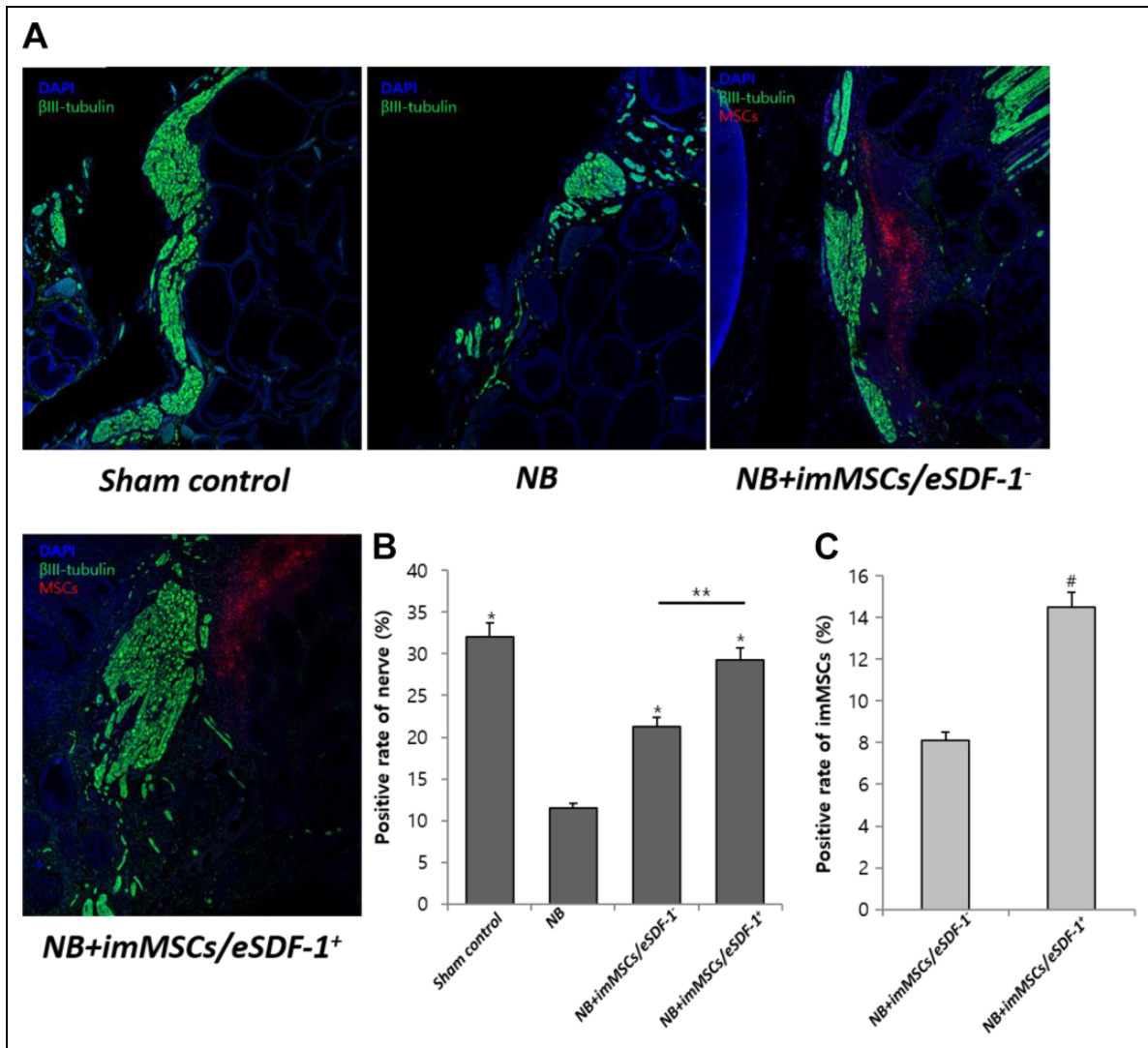


**Fig. 4.** MSC treatment accelerates the recovery of injured PN. (A) Representative images of PN staining in each group. Green is βIII-tubulin, blue is DAPI nucleus, and red is MSCs. Original magnification:  $\times 200$ . (B) Positive rate of nerve in each group. Each bar shows the mean values (standard deviation). \* $P < 0.01$  compared with NB group. \*\* $P < 0.05$  compared with NB+imMSCs/eSDF-1<sup>-</sup> group. (C) Positive rate of imMSCs in vivo. Each bar shows the mean values (standard deviation). # $P < 0.05$  compared with NB+imMSCs/eSDF-1<sup>-</sup> group. imMSC: immortalized mesenchymal stem cell; NB: neurogenic bladder; PN: pelvic nerve; SDF-1: stromal cell-derived factor-1.

mechanism. As shown in Figure 7, p-AKT/AKT and p-ERK/β-actin levels in the NB+imMSCs/eSDF-1<sup>-</sup> and NB+imMSCs/eSDF-1<sup>+</sup> group were higher ( $P < 0.05$ ), which suggested that after imMSC injection both PI3K/AKT/mammalian target of rapamycin (mTOR) and mitogen-activated protein kinase (MAPK) pathways were stimulated. Meanwhile, as shown in Figure 7, PN with higher SDF-1 expressed additional p-AKT and p-ERK to mediate the PI3K/AKT/mTOR and MAPK pathways ( $P < 0.05$ ).

## Discussion

Currently, the quality of life (QOL) during the postoperative period is of increasing concern<sup>15</sup>. QOL is an important aspect in the overall management of NB patients, for

example, to evaluate treatment-related changes in a patient<sup>16</sup>. Pelvic surgeries including radical prostatectomy, rectum resection, and hysterectomy are associated with a risk of PN injury<sup>17–19</sup>, which may trigger NB and subsequently lower the QOL postoperatively. Our results showed that NB decreased bladder function, reduced voided volume, and decelerate voiding frequency, which were ameliorated by imMSCs/eSDF-1. Obviously, QOL would be improved when NB was treated by imMSCs/eSDF-1. Li H et al.<sup>20</sup> illuminated that the regeneration of peripheral nerves after pelvic injury was a complex process involving neurons, Schwann cells, basal lamina, and end-organ responsiveness. Therefore, effective and potential treatments to recover the injured nerve and successfully cure NB are imperative. In this study, we established a rat model of NB and performed a

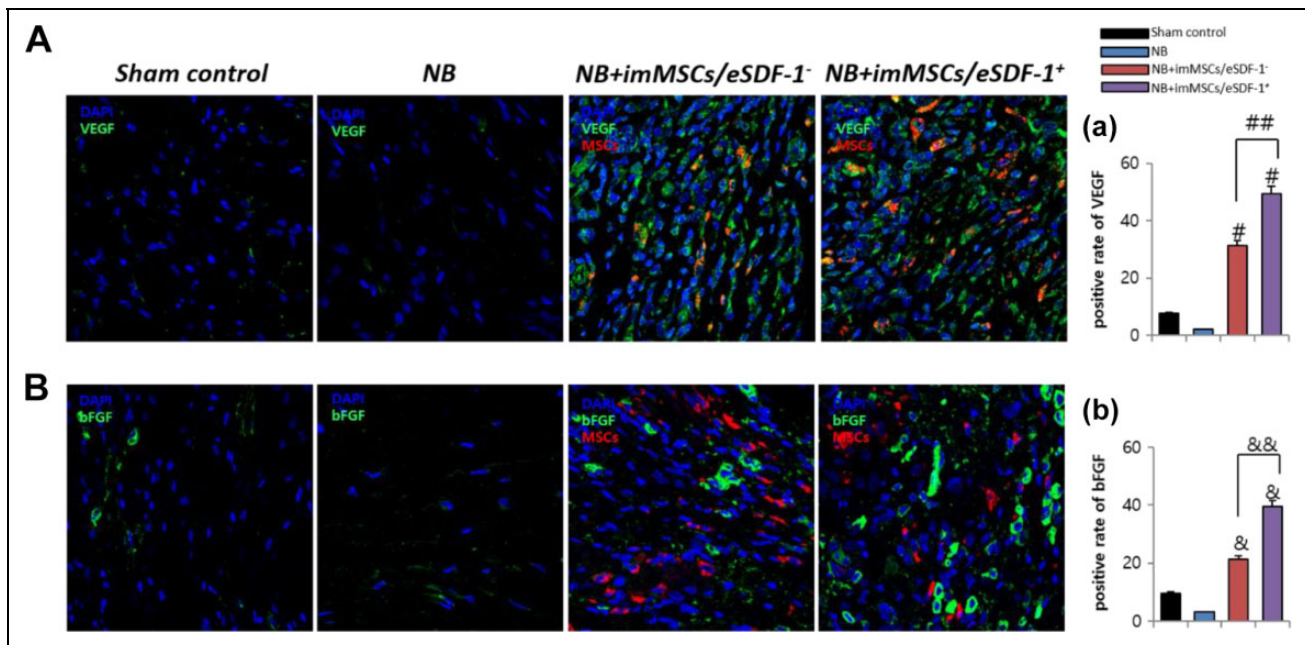


**Fig. 5.** SDF-1 improves VEGF and bFGF expression in vivo. (A) Representative images of VEGF stain for each group. Original magnification:  $\times 200$ . (a) Positive rate of VEGF for each group. Each bar shows the mean values (standard deviation).  $^{\#}P < 0.01$  compared with NB group.  $^{##}P < 0.01$  compared with NB+imMSCs/eSDF-1<sup>-</sup> group. (B) Representative images of bFGF stain for each group. Original magnification:  $\times 200$ . (b) Positive rate of bFGF for each group. Each bar shows the mean values (standard deviation).  $^{\&}P < 0.01$  compared with NB group.  $^{\&\&}P < 0.01$  compared with NB+imMSCs/eSDF-1<sup>-</sup> group. bFGF: basic fibroblast growth factor; imMSC: immortalized mesenchymal stem cell; NB: neurogenic bladder; SDF-1: stromal cell-derived factor-1; VEGF: vascular endothelial growth factor.

series of investigations with the imMSCs engineered. We found that imMSCs injection led to a significant elevation in the mean intravesical pressure of NB rats and an obvious thickening of the smooth muscle of bladder wall. Meanwhile, we found that in NB rats higher levels of SDF-1 in PN facilitated the recovery. We found that exposure to imMSCs ameliorated experimental NB dysfunction.

In a recent report<sup>21</sup>, investigators established a rat model of bilateral cavernous nerve crush injury. After stem cell injection, the expression of neural markers in the penile dorsal nerves and the erectile dysfunction improved significantly, suggesting that stem cells facilitate the repair of injured nerve. In a previous study<sup>14</sup>, we also found some similar outcomes in a rat model of diabetes mellitus erectile dysfunction. However, in both the studies, neurotrophic cytokines were merely detected. In our study, the imMSCs around the injured nerve were directly observed. Under increased SDF-1 levels produced by imMSCs, the restoration of nerve was steadily enhanced. Ouyang X et al.<sup>22</sup> reported that MSCs enhanced the recovery of the injured smooth muscle. They injected MSC-derived exosomes into the corpus cavernosum and after 4 weeks the recovery of the smooth muscles in corpus cavernosum was improved. However, few studies focused on bladder restoration and nerve recovery with MSC treatment. In our study, we found that the injection of imMSCs resulted in a thickening of bladder wall in NB rats markedly. We found that under a high SDF-1

microenvironment, the VEGF expression was also increased. VEGF is the key to tissue restoration. VEGF activated the PI3K-Akt signaling pathway, which increased the expression of nNOS during the recovery of injured nerve<sup>23,24</sup>. However, VEGF stimulated the MAPK signaling pathway to induce further p-ERK synthesis and activated the gene proliferation<sup>25</sup>.

Naderi-Meshkin et al.<sup>26</sup> demonstrated that SDF-1 played an important role in MSC homing. Fandel et al.<sup>27</sup> also reported stem cell homing to the PN after injection accompanied by high SDF-1 expression in the PN. In this study, we observed after imMSCs injection, several imMSCs migrated to the damaged nerve as the SDF-1 expression was upregulated. Our findings suggested that the increased SDF-1 expression led to further aggregation of imMSCs around the injured nerve. We supposed that MSCs also expressed SDF-1, which suggested a positive feedback, induced by SDF-1 expression in the injured nerve. Injured nerves expressed SDF-1 inducing migration of MSCs, which further expressed SDF-1, and upregulated the concentration of SDF-1 rapidly, resulting in enhanced migration of MSCs to the target tissue. To verify our hypothesis, we used a gene transfer technique, which facilitated imMSCs expression of higher levels of SDF-1 compared with normal imMSCs. Based on our results, we found that the quality of stem cells and the effect of MSC treatment yielded better outcomes in the



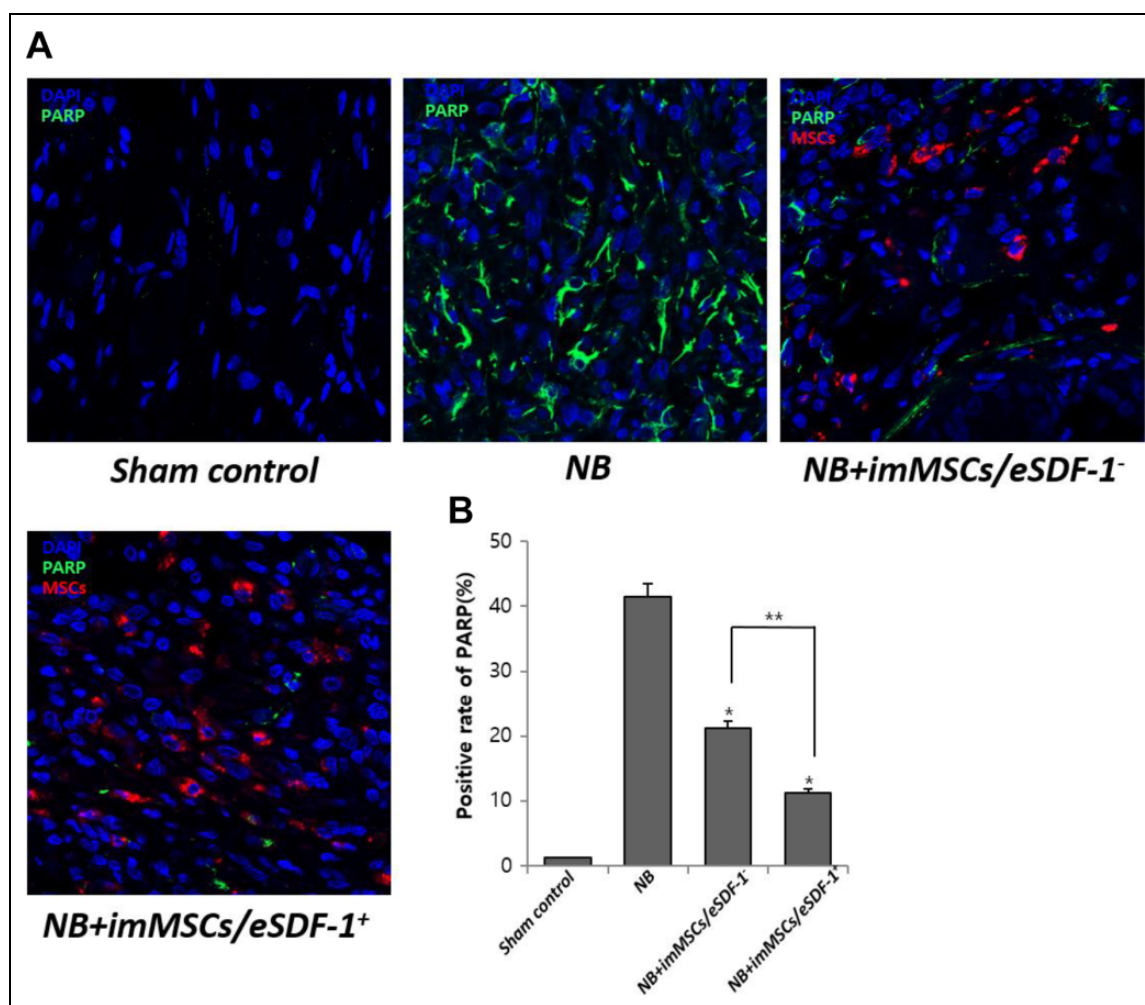


**Fig. 6.** MSCs degrade apoptosis by increasing the expression of SDF-1. (A) Representative images of apoptosis for each group. Original magnification:  $\times 200$ . (B) Positive rate of PARP for each group. Each bar shows the mean values (standard deviation). \* $P < 0.01$  compared with NB group. \*\* $P < 0.05$  compared with NB+imMSCs/eSDF-1<sup>-</sup> group. imMSC: immortalized mesenchymal stem cell; NB: neurogenic bladder; PARP: poly-ADP-ribose polymerase; SDF-1: stromal cell-derived factor-1.

upregulated SDF-1 group compared with the normal SDF-1 group, which validated our hypothesis of a positive feedback mediated via SDF-1 between injured nerves and MSCs. In this positive feedback, nerve injury triggered higher expression of MSCs and their directional migration. Zhou F et al.<sup>28</sup> believed that MSCs spread rapidly, upon injection, and only a few MSCs reached the target area. A few studies<sup>29</sup> considered that reactive oxygen species were toxic to injected stem cells due to the induction of apoptosis, which reduced the levels of MSCs rapidly. Both studies reported that the injected MSCs failed to remain at the injection site. However, the homing mechanisms of MSCs driven by SDF-1 explain the congregation of MSCs around the injured nerve. Meanwhile, we used the immortalized MSCs to prevent apoptosis of stem cells, to generate a stable microenvironment<sup>30</sup>. In brief, we eliminated other effects induced by MSCs and an unstable microenvironment. Under such

conditions, we demonstrated that imMSCs expressing a high level of SDF-1 had a positive effect on the restoration of injured nerves. The experiment involving MSC treatment was performed during an early stage of prostatitis.

There are still some defects in this article. First, we did not assess the viability of MSCs before injection, which decreased the accuracy of at least one part of the experiment. Comparing the viability before and after transfection, selection, and label would reduce errors by flow cytometry. Secondly, in the part of injured nerve regeneration, we just used the nerve staining and detection of nNOS expression. Adding a detection of some nerve biomarkers by a real-time polymerase chain reaction could make the results more convincing. At last, the mechanism research was not deep enough. So in the next study, we should focus on the pathway and factors to investigate the accurate mechanism of MSCs for NB.

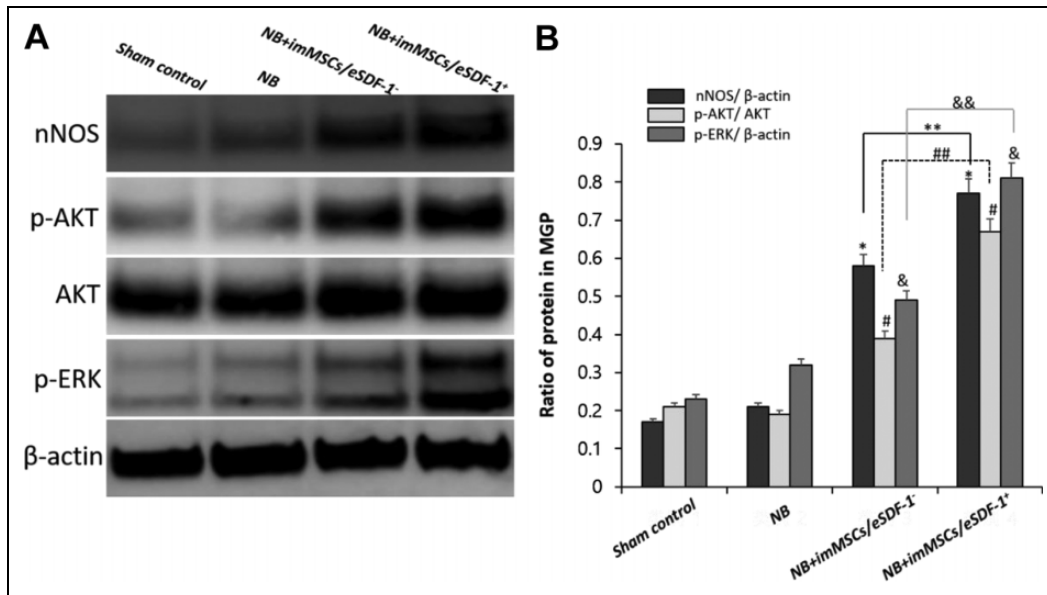


**Fig. 7.** (A) All groups were compared for nNOS, p-AKT, AKT, and p-ERK in PN by western blot. (B) Quantity analysis of western blot, including nNOS/β-actin, p-AKT/AKT, and p-ERK/β-actin. \* $P < 0.05$  compared with values from NB group. \*\* $P < 0.05$  compared with NB+imMSCs/eSDF-1<sup>-</sup> group. ## $P < 0.05$  compared with NB group. & $P < 0.05$  compared with NB group. && $P < 0.05$  compared with NB+imMSCs/eSDF-1<sup>-</sup> group. imMSC; immortalized mesenchymal stem cell; NB; neurogenic bladder; nNOS: neuronal nitric oxide synthase; PN: pelvic nerve; SDF-1: stromal cell-derived factor-1.

## Conclusions

The study demonstrated that high levels of SDF-1 expression induced rapid MSC homing to the target tissue and imMSCs/eSDF-1<sup>+</sup> improved NB by accelerating the restoration of injured nerves in a rat model. These experiments suggest a new therapeutic strategy using MSCs for NB, and, at least in part, provide a theoretic and experimental basis for clinical treatment.

## Authors' Contributions

Guan Qun Zhu, first author, was responsible for conception, study design, data analysis and interpretation, and manuscript writing. Seung Hwan Jeon was responsible for data collection and assembly, and data analysis. Kyu Won Lee and Hyuk Jin Cho were responsible for data collection and assembly. U Syn Ha, Sung Hoo Hong, and Eun Bi Kwon were responsible for providing the study material and animal models. Ji Youl Lee was responsible for conception and design, and data analysis and interpretation. Hyo-Jin Kim, Soon Min Lee, and Hey-Yon Kim were responsible for the design of cellular experiment. Woong Jin Bae and Sae Woong Kim, corresponding authors, were responsible for conception and design, financial support, drafting and revision of the manuscript, and final approval of the manuscript. All authors read and approved the final manuscript.

## Availability of Data and Materials

The datasets supporting the conclusions of this article are included in this article.

## Ethical Approval

This study was approved by the Institutional Animal Care and Use Committee of the Catholic University of Korea (CUMC-2016-0218-01).

## Statement of Human and Animals Rights

This article does not contain studies with human subjects. Animal experiments were reviewed and approved by the Institutional Animal Care and Use Committee of the Catholic University of Korea (CUMC-2016-0218-01).

## Statement of Informed Consent

There are no human subjects in this article and informed consent is not applicable.


## Declaration of Conflicting Interests

The author(s) declared no potential conflicts of interest with respect to the research, authorship, and/or publication of this article.

## Funding

The author(s) disclosed receipt of the following financial support for the research, authorship, and/or publication of this article: This research was supported by the Bio & Medical Technology Development Program of the National Research Foundation (NRF) funded by the Ministry of Science & ICT (NRF-2018M3A9E8020861)

## ORCID iD

Guan Qun Zhu  <https://orcid.org/0000-0001-7841-8026>

## References

1. Hoen L, Ecclestone H, Blok BF, Karsenty G, Phé V, Bossier R, Groen J, Castro-Diaz D, Padilla Fernández B, Del Popolo G, Musco S, et al. Long-term effectiveness and complication rates of bladder augmentation in patients with neurogenic bladder dysfunction: a systematic review. *Neurourol Urodyn*. 2017; 36(7):1685–1702.
2. Panicker JN, Fowler CJ, Kessler TM. Lower urinary tract dysfunction in the neurological patient: clinical assessment and management. *Lancet Neurol*. 2015;14(7):720–732.
3. Kim SJ, Lee DS, Bae WJ, Kim S, Hong SH, Lee JY, Hwang TK, Kim SW. Functional and molecular changes of the bladder in rats with crushing injury of nerve bundles from major pelvic ganglion to the bladder: role of RhoA/Rho kinase pathway. *Int J Mol Sci*. 2013;14(9):17511–17524.
4. Svihra J, Krhut J, Zachoval R, Svihrova V, Luptak J. Impact of clean intermittent catheterization on quality adjusted life years (QALYs) in spinal cord injury patients with neurogenic urinary incontinence. *Neurourol Urodyn*. 2017;37(1): 250–256.
5. Matthes SM, Reimers K, Janssen I, Liebsch C, Kocsis JD, Vogt PM, Radtke C. Intravenous transplantation of mesenchymal stromal cells to enhance peripheral nerve regeneration. *Biomed Res Int*. 2013;2013(15):573169.
6. Honmou O, Onodera R, Sasaki M, Waxman SG, Kocsis JD. Mesenchymal stem cells: therapeutic outlook for stroke. *Trends Mol Med*. 2012;18(5):292–297.
7. Osaka M, Honmou O, Murakami T, Nonaka T, Houkin K, Hamada H, Kocsis JD. Intravenous administration of mesenchymal stem cells derived from bone marrow after contusive spinal cord injury improves functional outcome. *Brain Res*. 2010;1343:226–235.
8. Yiou R, Hamidou L, Birebent B, Bitari D, Lecorvoisier P, Contremoulins I, Khodari M, Rodriguez AM, Augustin D, Roudot-Thoraval F, de la Taille A, et al. Safety of intracavernous bone marrow-mononuclear cells for postradical prostatectomy erectile dysfunction: an open dose-escalation pilot study. *Eur Urol*. 2016;69(6):988–991.
9. Zhu GQ, Jeon SH, Bae WJ, Choi SW, Jeong HC, Kim KS, Kim SJ, Cho HJ, Ha US, Hong SH, Kwon EB, et al. Efficient promotion of autophagy and angiogenesis using mesenchymal stem cell therapy enhanced by the low-energy shock waves in the treatment of erectile dysfunction. *Stem Cells Int*. 2018; 2018(1):1–14.
10. Liu TM, Ng WM, Tan HS, Vinitha D, Yang Z, Fan JB, Zou Y, Hui JH, Lee EH, Lim B. Molecular basis of immortalization of human mesenchymal stem cells by combination of p53 knockdown and human telomerase reverse transcriptase overexpression. *Stem Cells Dev*. 2012;22(2):268–278.
11. Gong M, Bi Y, Jiang W, Zhang Y, Chen L, Hou N, Liu Y, Wei X, Chen J, Li T. Immortalized mesenchymal stem cells: an alternative to primary mesenchymal stem cells in neuronal differentiation and neuroregeneration associated studies. *J Biomed Sci*. 2011;18(1):87.
12. Soler R, Füllhase C, Santos Andersson KE. Development of bladder dysfunction in a rat model of dopaminergic brain lesion. *Neurourol Urodyn*. 2011;30(1):188–193.
13. Eeyne E, Dewulf K, Deruyter Y, Rietjens R, Everaerts W, Bivalacqua TJ, De Ridder D, Van der Aa F, Albersen M. Characterization of voiding function and structural bladder changes in a rat model of neurogenic underactive bladder disease. *Neurourol Urodyn*. 2018;37(5):1594–1604.
14. Jeon SH, Shrestha KR, Kim RY, Jung AR, Park YH, Kwon O, Kim GE, Kim SH, Kim KH, Lee JY. Combination therapy using human adipose-derived stem cells on the cavernous nerve and low-energy shockwaves on the corpus cavernosum in a rat model of post-prostatectomy erectile dysfunction. *Urology*. 2016;88:226. e1–9.
15. Eveno C, Lamblin A, Mariette C, Pocard M. Sexual and urinary dysfunction after proctectomy for rectal cancer. *J Visc Surg*. 2010;147(1):e21–e30.
16. Groen J, Pannek J, Castro Diaz D, Del Popolo G, Gross T, Hamid R, Karsenty G, Kessler TM, Schneider M, 't Hoen L, Blok B. Summary of European association of urology (EAU) guidelines on neuro-urology. *Eur Urol*. 2016;69(2):324–333.
17. Matsukawa Y, Hattori R, Komatsu T, Funahashi Y, Sassa N, Gotoh M. De novo detrusor underactivity after laparoscopic radical prostatectomy. *Int J Urol*. 2010;17(7):643–648.
18. Lange MM, Maas CP, Marijnen CA, Wiggers T, Rutten HJ, Kranenbarg EK, van de Velde CJ. Cooperative clinical investigators of the Dutch total mesorectal excision trial. Urinary dysfunction after rectal cancer treatment is mainly caused by surgery. *Br J Surg*. 2008;95(8):1020–1028.
19. Nitta M, Tamaki T, Tono K, Okada Y, Masuda M, Akatsuka A, Hoshi A, Usui Y, Terachi T. Reconstitution of experimental neurogenic bladder dysfunction using skeletal muscle-derived multipotent stem cells. *Transplantation*. 2010;89(9):1043–1049.
20. Li H, Matheu MP, Sun F, Wang L, Sanford MT, Ning H, Banie L, Lee YC, Xin Z, Guo Y, Lin G, et al. Low-energy shock wave therapy ameliorates erectile dysfunction in a pelvic neurovascular injuries rat model. *J Sex Med*. 2016;13(1):22–32.
21. Yang Q, Chen X, Zheng T, Han D, Zhang H, Shi Y, Bian J, Sun X, Xia K, Liang X, Liu G, et al. Transplantation of human urine-derived stem cells transfected with pigment epithelium-derived factor to protect erectile function in a rat model of cavernous nerve injury. *Cell Transplant*. 2016;25(11): 1987–2001.
22. Ouyang X, Han X, Chen Z, Fang J, Huang X, Wei H. MSC-derived exosomes ameliorate erectile dysfunction by alleviation of corpus cavernosum smooth muscle apoptosis in a rat model of cavernous nerve injury. *Stem Cell Res Ther*. 2018; 9(1):246.
23. Fujiki M, Abe E, Nagai Y, Shiqi K, Kubo T, Ishii K, Abe T, Kobayashi H. Electroconvulsive seizure-induced VEGF is correlated with neuroprotective effects against cerebral infarction: involvement of the phosphatidylinositol-3 kinase/Akt pathway. *Exp Neurol*. 2010;225(2):377–383.
24. Chen X, Yang Q, Zheng T, Bian J, Sun X, Shi Y, Liang X, Gao G, Liu G, Deng C. Neurotrophic effect of adipose tissue-derived stem cells on erectile function recovery by pigment

- epithelium-derived factor secretion in a rat model of cavernous nerve injury. *Stem Cells Int.* 2016;2016:5161248.
25. Harding A, Cortez-Toledo E, Magner NL, Beegle JR, Coleal-Bergum DP, Hao D, Wang A, Nolta JA, Zhou P. Highly efficient differentiation of endothelial cells from pluripotent stem cells requires the Mapk and the PI3 K pathways. *Stem Cells.* 2017;35(4):909–919.
  26. Naderi-Meshkin H, Matin MM, Heirani-Tabasi A, Mirahmadi M, Irfan-Maqsood M, Edalatmanesh MA, Shahriyari M, Ahmadiankia N, Moussavi NS, Bidkhori HR, Bahrami AR. Injectable hydrogel delivery plus preconditioning of mesenchymal stem cells: exploitation of SDF-1/CXCR4 axis toward enhancing the efficacy of stem cells' homing. *Cell Biol Int.* 2016;40(7):7307–7341.
  27. Fandel TM, Albersen M, Lin G, Qiu X, Ning H, Banie L, Lue TF, Lin CS. Recruitment of intracavernously injected adipose-derived stem cells to the major pelvic ganglion improves erectile function in a rat model of cavernous nerve injury. *Eur Urol.* 2012;61(1):201–210.
  28. Zhou F, Hui Y, Xu Y, Lei H, Yang B, Guan R, Gao Z, Xin Z, Hou J. Effects of adipose-derived stem cells plus insulin on erectile function in streptozotocin-induced diabetic rats. *Int Urol Nephrol.* 2016;48(5):657–669.
  29. Liu GY, Jiang XX, Zhu X, He WY, Kuang YL, Ren K, Lin Y, Gou X. ROS activates JNK-mediated autophagy to counteract apoptosis in mouse mesenchymal stem cells in vitro. *Acta Pharmacol Sin.* 2015;36(12):1473–1479.
  30. Liu MC, Chen WH, Chiou CS, Lo WC, Dubey NK, Chen YC, Lai WT, Yeh SD, Chiang HS, Deng WP. Inhibition of chronic prostate inflammation by hyaluronic acid through an immortalized human prostate stromal cell line model. *PLoS One.* 2017; 12(5):e0178152.